Tripropellant Engine Technology for Reusable Launch Vehicles

N. S. Gontcharov,* V. A. Orlov,† V. S. Rachuk,‡ M. A. Rudis,§ and A. V. Shostak¶
Chemical Automatics Design Bureau, Voronezh, Russia

and

R. G. Starke** and J. R. Hulka††
Aerojet General Corporation, Sacramento, California

Nomenclature

c^* = characteristic exhaust velocity, m/s
E = modulus of elasticity, MPa
H = pump head, m
H_2 = hydrogen
k = kerosene
l_{ak} = amplitude of elasto-plastic deformation
l_f = ultimate deformation in stress concentration area
$\dot{m}$ = mass flow rate, kg/s
$\bar{m}$ = relative mass flow rate
m_o = low cycle fatigue curve exponent
m_e = low cycle fatigue curve exponent

*Vice President.
†Doctor of Technical Science, Head of Department.
‡Doctor of Technical Science, President.
§Doctor of Technical Science, Head of Structural Analysis Department.
¶Head of Design Bureau.
**Chief Project Engineer.
††Engineering Specialist; currently with Jacobs/Sverdrup Technology. Senior Member AIAA.

N_e = number of operational cycles or engine cycles
N_o = number of cycles before crack initiation
O_2 = oxygen
p = pressure, MPa
r = mixture ratio
R = gas constant, (kgf · m)/(kg · def K)
T = temperature, K
ΔV = vehicle velocity increment, m/s

Greek

β = stress loading cycle asymmetry factor
β_* = strain loading cycle asymmetry factor
Ψ = relative cross-sectional area reduction
σ_B = ultimate strength of material, MPa
σ_{-1} = fatigue limit of material, MPa
η_N = durability margin factor
ρ = density, kg/m^3

Subscripts

e = experimental
g = gas generator (preburner)
H = hydrogen
k = kerosene
m = main (main combustion chamber)
nom = nominal
o = oxidizer
p = predicted

Superscripts

H = (hydrogen) fuel-rich
O = oxidizer-rich

I. Introduction

AFTER 70 years of development, rocket vehicles have reached a level of sophistication where cost is the deciding factor. Designers of the next generation of launch vehicles must dramatically reduce the costs for transportation of payloads to orbit, while improving vehicle reliability, operability, and efficiency. Cost drivers include the size of the vehicle, the size and weight of the payload, the inclusion of human pilots and passengers, the number of stages, the number of propellants on board, the landing mode, the materials of construction, the reusability of the vehicle, and the propulsion system.

A NASA space transportation architecture study[1,2] examined medium payload class, one-stage and two-stage launch vehicles where different takeoff and landing criteria resulted in vehicles of varying designs. A reusable launch vehicle (RLV) was selected as the baseline vehicle that, used with an interim expendable launch fleet, would offer significant reductions in annual operating costs over existing vehicles.[1,2] In theory, reusable vehicles have the lowest life cycle costs, although

they may also have the highest initial costs and therefore are the most sensitive to variable fiscal policies.

Most space transportation operation cost studies, including the NASA study, also favor the one-stage, or single-stage-to-orbit (SSTO) rocket vehicle, for the simple reason that multiple stages require multiple pieces of hardware that need procurement, servicing, assembly, integration, and maintenance. These cost factors generally outweigh the advantages of two-stage systems that may be smaller and lighter, and also less sensitive to weight growth.[3] In addition, SSTO vehicles have no expendable hardware components that would add to the debris in space, no additional stages required to be returned to the launch site, and in theory the most minimal servicing, resulting in the fastest response and shortest turnaround time to flight.

Design features of this ultimate SSTO vehicle have been the subject of debate over the past 40 years, however. Although many concepts have been generated, until recently none has been shown to be technically feasible with the technologies available at the time, due to a combination of issues such as insufficient engine performance, excessive engine and vehicle size and weight, and high development costs. Many early SSTO studies concluded that vehicles designed then could not theoretically deliver a payload into orbit. A primary difficulty is the propulsion—that is, of configuring a lightweight system that emulates booster engine characteristics at low altitude and upper-stage engine characteristics for ascent and orbit insertion.[4,5]

One of the most important theoretical advancements to improve feasibility of SSTO vehicles was the introduction of mixed-mode propulsion by Salkeld,[6] in which different modes of propulsion with different propellant densities were combined in the same stage. Salkeld initially concluded that the optimum burn profile to maximize ideal ΔV for a two-mode, single-stage rocket vehicle was purely sequential, with the higher specific-density impulse mode operating first in the boost portion of the flight, and the higher specific-impulse mode operating during the ascent portion of the flight.[6] Many rocket vehicles already operated this way, in fact, by using the different modes in different stages, although the individual propulsion modes were optimized for each stage.

However, carrying hydrogen engines or engine components without using them at liftoff appeared to create a penalty on vehicle or engine mass.[7] Studies showed that various engine types on a vehicle with parallel burn (i.e., simultaneous operation of hydrocarbon and hydrogen at liftoff) could provide vehicle dry mass and gross liftoff weight at least as good as that of a vehicle with series burn.[7–9] One of the important advantages of a parallel burn vehicle is that the hydrogen engine or engine components can be ignited on the ground and thus can be monitored and evaluated before liftoff, an obvious increase in vehicle reliability.

Since the introduction of the mixed-mode principle to SSTO vehicle propulsion, there have been numerous studies that showed that a mixed-mode or dual-fuel SSTO vehicle has many distinct advantages over reference single-fuel SSTO vehicles.[3,7,9–14] The main benefit of the mixed-mode operation results from the fact that most of the propellant is burned in achieving a relatively small percentage of the velocity to orbit and is maximized by burning the high-density fuel early in the flight. When a high-density propellant combination is burned in this initial phase of the flight, the resultant vehicle size and dry weight are less

for a fixed payload mass. The vehicle size and dry weight are historically considered to be roughly representative of both the development, test, and engineering (DT&E) costs and the life cycle costs (LCC) of a vehicle. Dry weight is the weight of the vehicle without propellant, fluids, payload, or crew.

The tripropellant engine concept is in fact a self-contained mixed-mode engine, where the first operating mode, for liftoff on the ground, is tripropellant (hydrocarbon, liquid hydrogen, and liquid oxygen), and the second operating mode, for sustain performance at altitude, is bipropellant (liquid hydrogen and liquid oxygen). A tripropellant engine such as this retains all of the benefits of the mixed-mode principle for the launch vehicle and has additional engine and vehicle benefits. The availability of hydrogen for cooling significantly increases the allowable chamber pressure for hydrocarbon fuel-rich turbine drive systems, and hence increases performance and reduces engine size, since there is no reliance on the hydrocarbon fuel or the oxygen for chamber wall or nozzle cooling. By shutting off the kerosene flow, the tripropellant engine is transformed into a bipropellant liquid oxygen/hydrogen engine, achieving the mixed-mode benefit with a single barrel engine, which will reduce the rear panel or "boat tail" area of SSTO launch vehicles, reducing vehicle weight and improving aerodynamic efficiency by moving the vehicle center of gravity forward. By initiating the hydrogen flow and ignition on the launch pad, there is no reliance on upper atmosphere chilling and ignition of a staged or serial burn engine, which would add system weight for the storage of purge gases and may reduce vehicle reliability.

Mixed-mode vehicle studies performed with separate hydrocarbon-fueled and hydrogen-fueled engines showed that vehicle dry weight could be reduced 30% over an all-hydrogen reference vehicle.[7,11] With dual fuel engines, vehicle dry weight could be reduced 35–50%.[3,7,11] Specific tripropellant engine studies[3,15] considered many advanced concepts available at the time, all integrating the turbopumps and using hydrogen for cooling, but using different drive gas and piping schemes and nozzle concepts. All these studies found they could reduce the vehicle dry weight of a reference all-hydrogen SSTO vehicle, ranging from a 21% reduction with a hydrogen gas generator tripropellant engine design, to over 30% reduction for dual bell and dual expansion engine designs. Tripropellant in this instance refers to a dual fuel scheme because the two fuels, hydrogen and a hydrocarbon, share a common oxidizer, oxygen.

However, in one study, a clean-sheet LO_2/LH_2 engine provided more dry weight reduction (primarily by increasing mixture ratio from 6.0 to 6.9) than a clean-sheet tripropellant engine.[16] With advances in other areas of SSTO vehicle technology, or if clean-sheet engines are considered, the use of tripropellant engines may not be critical to the development of an SSTO vehicle.[1,16,17] The large weight penalties on the vehicle due to the low density of hydrogen, because of larger tanks and feed structures, can be reduced by the proposed use of lightweight advanced composite materials, so that performance from single fuel engines becomes feasible. Preliminary designs have been developed of an SSTO vertical-takeoff, horizontal-landing (VTHL) vehicle that delivers a 9100-kg payload to a Space Station Freedom orbit, using only single mixture ratio, all-hydrogen propulsion, with dry weight growth margin of 15%.[17]

Whether this vehicle dry weight growth margin is adequate is debatable, given that the space shuttle weight growth was 25%.[1] Many vehicle and engine

performance issues still remain that create doubts about vehicle dry weight gain, and cost issues remain because of engine reusability. Consequently, continued studies of additional technologies, including a tripropellant engine, were recommended that would provide additional vehicle dry weight reduction.[1] The use of tripropellant engines, by reducing the dry weight of the vehicle, provides for an increase in the dry weight growth margin.[1]

In the NASA study, an all-hydrogen vehicle was chosen based on an evolved engine because of the potential savings in engine development costs.[1] However, continued evaluation of tripropellant engines was recommended due to vehicle dry weight savings and weight growth margin increase. One tripropellant engine considered was also an evolved engine, based on the existing Russian liquid oxygen/kerosene propellant RD-170 engine. The RD-170 engine is a flight-qualified engine that supplied the main propulsion for the booster core stage of the Energia heavy-lift launch vehicle.[18,19] A tripropellant engine concept based on the RD-170 engine, the RD-701, was developed in Russia for the Multipurpose Aerospace System (MAKS).[20] This two-stage-to-orbit space plane was to be air launched from a Russian AN-225. The RD-701 went through complete mechanical design and analysis, including systems integration with the MAKS space plane, before the program was postponed in 1991.[20]

The RD-701 engine uses a significant portion of the RD-170, including the same oxidizer-rich preburner cycle. The preburner is unchanged, while all the hydrogen is used in the main combustion chamber for coolant. The main injector is modified to include injection of the hydrogen from the main combustion chamber. Initial subscale development testing of the tripropellant main injector shows that high performance can be achieved with three propellants,[21] which is corroborated by numerous other studies.[22–32]

A tripropellant engine can also be developed with a fuel-rich preburner cycle. In this chapter, an evolved tripropellant engine is discussed based on another existing Russian engine, the liquid oxygen/hydrogen propellant RD-0120 engine, which operates with a fuel-rich turbine drive gas. The RD-0120 engine is a flight-qualified engine that supplied the main propulsion for the sustainer core stage of the Energia heavy-lift launch vehicle.[33] Under a typical flight profile, it was ignited at sea level and operated 460 s, producing a nominal vacuum thrust of 200 metric tons and a vacuum delivered specific impulse of 455.5 s.[33] The RD-0120 engine completed extensive qualification testing, with more than 163,000 s of testing accumulated on more than 90 engines prior to the first flight, and has a demonstrated reliability of 0.992 at 90% confidence.[33] A tripropellant engine based on this highly evolved engine also would include substantial development savings.

In this chapter, the design and development issues of a tripropellant liquid rocket engine using a closed (or staged combustion) power cycle and a fuel-rich propellant turbine drive gas scheme are discussed. The first section reviews issues for selection of the tripropellant engine turbine drive gas. Next, the optimum configuration of the turbine drive gas engine is reviewed, followed by discussion of the main technical issues this engine will face to be used on an SSTO RLV. Finally, a demonstration tripropellant engine program using the liquid oxygen/liquid hydrogen RD-0120 as a test bed is briefly described, illustrating that many of these issues can be investigated in a cost-effective fashion.

II. Selection of Tripropellant Engine Cycle for Reusable SSTO Application

The SSTO RLV application places many significant requirements on the engines, of which the most important is reusability. To be cost effective in a reusable vehicle, the engine must withstand typically 25 starts over an operating duration of 12,500 s between refurbishment. Total operating life would be typically 125 starts over a total operating duration of 62,500 s. In addition, the engine must also be high performing and low weight, otherwise its inclusion on the SSTO vehicle would result in pound-for-pound payload deductions and reduced vehicle stability.

There are several variants of engine schemes to be considered that may meet these requirements. The most widely recognized is the staged combustion cycle, with full or partial secondary combustion of the gas from the preburner. In this section, the schemes for two different partial secondary combustion tripropellant schemes are compared. One has an oxidizer-rich turbine drive generated by a bipropellant preburner, along with hydrogen cooling of the chamber and nozzle, and a main chamber injector with liquid/gas/gas propellant injection. The other has a fuel-rich turbine drive generated by a tripropellant preburner, along with hydrogen cooling of the chamber and nozzle, and a main chamber injector with liquid/gas propellant injection. Full secondary combustion, using both fuel-rich and oxidizer-rich gas to drive separate turbines, offers potential advantages over either of these schemes, such as the elimination of unlike propellant pump and drive gas schemes, but also has disadvantages, such as increased control complexity. For brevity, this scheme is not considered in this chapter. However, the advantages and disadvantages of each partial secondary combustion scheme may be weighed for the full combustion scheme.

All the tripropellant engines are dual mode: one mode with hydrocarbon/hydrogen flow for high specific density impulse during liftoff, and the other mode with hydrogen-only flow for high specific impulse for ascent into orbit. Based on one vehicle optimization in Russia for maximizing payload, the ratio of the thrust level of the first mode to the second mode is approximately 2.5. For the example applied in this chapter, vacuum thrust levels per engine at these modes are estimated as 200 and 80 metric tons, respectively, noting that the sea-level thrust per engine must exceed 150 metric tons for typical vehicles.

A. Turbine Drive Power of Preburner Gas

The first important comparison is the ratio of available power or work capability of the turbine drive gas. Table 1 shows the parameters used to calculate the relative power (or work capability) $\dot{m}_g R_g T_g$ of the following three preburner gas compositions: 1) bipropellant oxidizer-rich preburner gas (kerosene and liquid oxygen), 2) tripropellant fuel-rich preburner gas (kerosene, liquid hydrogen, and liquid oxygen), and 3) bipropellant fuel-rich preburner gas (liquid hydrogen and liquid oxygen). The parameters shown are for various gas temperatures and engine propellant mixture ratios r_m, where $\bar{m}_g = \dot{m}_g/\dot{m}$. To calculate

Table 1 Calculation of turbine power for three preburner gas compositions

Propellant composition	Parameter	Units	H_2, 6%; kerosene, 12.6%; O_2, 81.4%			H_2, 5%; kerosene, 14%; O_2, 81%			H_2, 4%; kerosene, 15.6%; O_2, 80.4%		
Tripropellant fuel-rich	r_m	—	4.376			4.263			4.102		
	$\bar{m}_g$	—	0.294	0.310	0.321	0.286	0.310	0.320	0.279	0.296	0.307
	R_g	$\frac{kg_f - m}{kg - K}$	122.5	121.5	119.5	107.3	107.1	107.0	91.4	93.5	94.5
	r_g	—	0.581	0.667	0.726	0.505	0.632	0.684	0.423	0.510	0.564
	T_g	K	850	950	1000	850	950	1000	850	950	1000
	$\bar{m}_g R_g T_g$	$\frac{kg_f - m}{kg}$	30610	35780	38360	26090	31520	34240	21680	26310	28960
Bipropellant fuel-rich	$\bar{m}_g$	—	0.093	0.099	0.102	0.078	0.083	0.085	0.062	0.066	0.068
	R_g	$\frac{kg_f - m}{kg - K}$	273	256	249	273	256	249	273	256	249
	r_g	—	0.55	0.65	0.70	0.55	0.65	0.70	0.55	0.65	0.70
	T_g	K	850	950	1000	850	950	1000	850	950	1000
	$\bar{m}_g R_g T_g$	$\frac{kg_f - m}{kg}$	21580	24080	25400	17980	20060	21170	14387	16050	16930
Bipropellant oxidizer-rich	$\bar{m}_g$	—	0.833	0.835	0.836	0.829	0.831	0.832	0.822	0.825	0.826
	R_g	$\frac{kg_f - m}{kg - K}$	26.6	26.6	26.6	26.6	26.6	26.6	26.6	26.6	26.6
	r_g	—	43.63	38.67	36.70	43.63	38.67	36.7	43.63	38.67	36.70
	T_g	K	850	950	1000	850	950	1000	850	950	1000
	$\bar{m}_g R_g T_g$	$\frac{kg_f - m}{kg}$	18830	21100	22240	18740	20100	22130	18590	20840	21970

the preburner gas flow rates, the following equation was applied:

$$r_m = \bar{m}_o/(\bar{m}_k + \bar{m}_h) \tag{1}$$

where $\bar{m}_h$, $\bar{m}_k$, and $\bar{m}_o$ are the relative flow rates of liquid hydrogen, kerosene, and liquid oxygen, respectively, defined as $\bar{m}_i = \dot{m}_i/\dot{m}$, and $\dot{m}$ is the sum of $\dot{m}_h$, $\dot{m}_k$, and $\dot{m}_o$. The propellant flow rates through the preburner are defined by the following equations:

$$\bar{m}_g = \frac{r_m}{1 + r_m} \cdot \frac{1 + r_g}{r_g} \tag{2}$$

where $r_g = \dot{m}_o/\dot{m}_{kg}$, for the bipropellant preburner with the oxygen-rich gas;

$$\bar{m}_g = \frac{1 + r_g}{1 + r_m} \tag{3}$$

where $r_g = \dot{m}_{og}/(\dot{m}_k + \dot{m}_h)$, for the tripropellant preburner with the fuel-rich gas; and

$$\bar{m}_g = \bar{m}_h \cdot (1 + r_g) \tag{4}$$

where $r_g = \dot{m}_{og}/\dot{m}_h$, for the bipropellant preburner with the fuel-rich gas, and where $\bar{m}_h = \dot{m}_h/\dot{m}$ is the relative flow rate of hydrogen.

Comparison of the $\bar{m}_g R_g T_g$ parameters given in Table 1 shows that the relative power of the preburner gas for the fuel-rich scheme applied to the tripropellant preburner, over a gas temperature range of 850–1000 K and at different mixture ratios (i.e., different hydrogen percentages for tripropellant), is 1.72 to 1.17 times higher than for the oxidizer-rich preburner scheme with a tripropellant engine application, and 1.42 to 1.71 times higher than for the bipropellant fuel-rich preburner scheme. These ratios are illustrated in Fig. 1. However, if the main thrust chamber pressures for all the schemes are equal, the tripropellant or the bipropellant fuel-rich scheme requires 1.1 times more turbomachinery power than that for the oxidizer-rich scheme, because the hydrogen must be pumped to a higher pressure to supply the preburner. Therefore, from consideration of the overall utilization of energy in the engine, the fuel-rich scheme for the tripropellant preburner has more relative power than the oxidizer-rich scheme by 1.48 to 1.56 times for the fuel that has 6% hydrogen, and 1.06 to 1.20 times for the fuel with 4% hydrogen, over the preburner gas temperature range of 850–1000 K.

Consequently, considering the energy utilization for the tripropellant engine in the first mode, the tripropellant fuel-rich preburner scheme has advantages in lower preburner gas temperature at the same chamber pressure, or higher chamber pressure at the same preburner gas temperature, than the oxidizer-rich scheme, as shown in Fig. 2. To reach the same chamber pressure of 24.5 MPa for the propellants with 6% hydrogen, the preburner gas temperature with the oxidizer-rich scheme must increase by 200 K. Conversely, at the same preburner gas

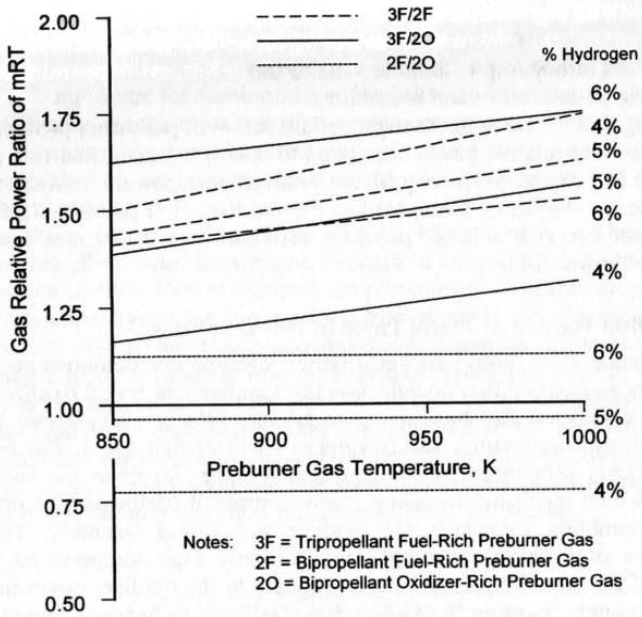

Fig. 1 Comparison of relative turbine drive gas power capability.

temperature of 850 K, the fuel-rich scheme attains a chamber pressure approximately 5 MPa higher. These calculations illustrate that a tripropellant engine with a tripropellant preburner will either 1) provide an increase of specific impulse by 3–4 s in the tripropellant mode, assuming a fixed nozzle exit diameter (or engine envelope), and hence reduce the engine weight as the chamber

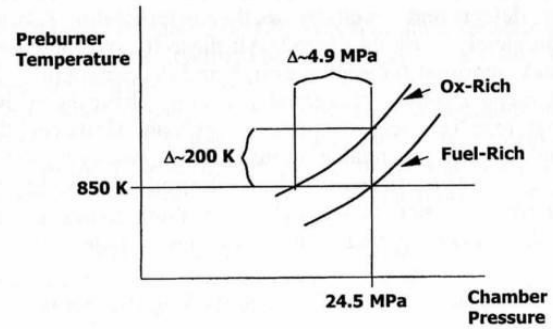

Fig. 2 Comparison of fuel-rich and oxidizer-rich turbine drive gas schemes for generation of turbine power, with 6% hydrogen propellant in engine.

pressure will be higher with the same nozzle exit diameter, at the same preburner temperature; or, 2) at the same chamber pressure, will lower the internal stresses on ducts and turbopump assemblies due to the lower gas temperatures and thus provide higher reliability and reusability.

The engine scheme with the tripropellant fuel-rich preburner provides 1.42 to 1.71 times more relative power compared to the bipropellant fuel-rich preburner (hydrogen and oxygen). The required turbomachinery powers for these two cases are practically the same. Compared to the oxidizer-rich preburner scheme, the bipropellant fuel-rich scheme provides 1.14 more to 0.77 times less relative power, as shown in Fig. 1.

B. Ignition Hazard of Metal Parts in Hot Gas Flow

Experience from liquid rocket engine development demonstrates that the assemblies and piping that contain flowing gaseous and liquid oxidizer provide the most significant fire hazard in the engine. Nearly every metal has some finite kindling temperature with oxygen or oxidizer-rich gases. The fire hazard is significantly influenced by the heat and pressure levels in the engine components, which result in increasing stressed-strained (deformed) characteristics of the assemblies, especially the oxidizer turbopump assembly. There have been cases of burning resulting from not only high temperatures but also rubbing of the metallic parts of the turbopump in the oxidizer environment.

Unfortunately, burning in oxidizer-rich gas ducts or turbines cannot be satisfactorily predicted because many unpredictable factors may cause ignition, including: 1) the appearance of microcracks in the material; 2) the appearance of metallic particles from the engine cavities and turbine cavities and gaps between the movable and unmovable parts of the turbopump assembly, which under conditions of high temperature and pressure in the oxidizing environment will ignite and spur ignition of the environment; and 3) rubbing of movable assemblies and unmovable housings because of e.g., deformation of rotor housings. The use of oxidizer-rich turbine gas for reusable engine applications presents a loss of reliability due to the increase of fire hazard in the engine. Also, the development program for the engine designed with the oxygen-rich staged combustion cycle may be more costly because test failures do not provide enough data on defects and deviations, as the corresponding hardware elements are usually completely burnt and fused. All these factors increase the cost and lengthen the time required for engine design and development.

To prevent metal ignition, nonignitable coatings have been used to protect those parts that may be most sensitive to ignition. However, these coatings have been developed for expendable liquid rocket engine components. For a reusable application, use of these coatings is not desired because they may be pitted or removed during repeated or extensive operation, requiring inspection and repairs that will increase the operation costs of the vehicle.

C. Preburner Temperature for Reusability Requirements

The reusability requirement is the basis for establishment of the engine operating parameters, most especially for the selection of the proper temperature of the preburner gas. Numerous hot-fire tests conducted on engines with long life,

as well as studies of the material properties at cyclic loading, provided for the development of the philosophy and principles of durability estimations for the most stressed assemblies of the engine.[34] The temperature of the preburner gas is a determining factor for turbine blade durability and for engine life because the turbine blades are the most sensitive engine components. This section evaluates the maximum temperatures required to satisfy the reusability and life requirements (but do not take into account the additional fire hazard of the oxidizer-rich gas piping).

Studies have been conducted for turbine blades made of heat-resistant chrome-nickel alloy, with the ultimate strength of $\sigma_B \geq 1225$ MPa, and relative area reduction of $\Psi \geq 15\%$ at ambient temperatures.[34] Reusable engine assemblies operate under cyclic loading resulting from thermal variations and mechanical vibrations during the startup and shutdown transients of the engine. Such cyclic loading leads to material low-cycle fatigue, crack initiation in stress concentration areas, and, subsequently, assembly failure. At a low number of loading cycles, the loads may exceed the yield strength, and so the estimations of the elasto-plastic deformation range Δl_k and the amplitude of the elasto-plastic deformations $l_{ak} = \Delta l_k/2$ are important. The amplitude of elasto-plastic deformation l_{ak} relates to the number of cycles until crack initiation, N_o, as

$$l_{ak} = \frac{l_f^T}{2(4N_o)^{m_o} + \beta_*} + \frac{\sigma_B^T/E^T}{(4N_o)^{m_e} + \beta} \tag{5}$$

In this dependence, l_f is an ultimate (destructive) deformation of the material in the stress concentration area and is determined considering the three-dimensional stressed state and the environmental effect (particularly, hydrogen) on the material mechanical properties. The low cycle fatigue curve exponents m_o and m_e reflect the strength and durability characteristics, σ_B^T and σ_{-1}^T, respectively, as

$$m_o = 0.36 + 0.002\sigma_B^T \tag{6}$$

$$m_e = 0.15\log(\sigma_B^T/\sigma_{-1}^T) \tag{7}$$

We can assume that $\beta_* \cong 0$ and $\beta \cong 1.0$. Note that the dependence $l_{ak}(N_o)$ corresponds to the "overstressed" loading conditions ($\Delta l_k \cong$ constant), which as a rule occurs in stress concentration areas.

The calculations just described were conducted for a preburner gas temperature range of 973–1123 K. The formations of the stress concentration areas on the blades as a result of the blade design and manufacturing peculiarities were taken into account. The blades are exposed to the transient heat loads, which are of primary importance in these studies.

As the preburner gas temperature and consequently the blade temperature rises, the elasto-plastic deformations magnify significantly, especially in stress concentration areas. This reduces the material strength properties and shortens blade durability. Based on the structural analysis calculations at a preburner gas temperature of 973 K, the number of cycles prior to the crack initiation in the stress concentration areas is $N_o \sim 180$. At a preburner gas temperature of

1123 K, the number of cycles prior to the crack initiation is $N_o \sim 19$. The most significant durability decrease is observed at the temperature range of the preburner gas from 1023 to 1173 K. Figure 3 presents the results of these calculations. The number of cycles to crack initiation, N_o, is considered to be the limit. Thus, to determine the number of the operational cycles N_e, the durability margin factor η_N is introduced as follows:

$$\eta_N = N_o/N_e \tag{8}$$

Though currently the durability margin factor is taken as $\eta_N = 4$, the durability margin is considered to decrease as the number of load cycles rises.

Experience has shown that taking $\eta_N = 4$ substantially overestimates durability margin.[34] Furthermore, the constant value of η_N, which does not depend on the number of operating cycles N_e, may result in high durability requirements that can hardly be realized in practice.

The durability margin factor η_N should be a function of N_e, such that increasing N_e should decrease η_N. The approach to the determination of η_N that connects the number of loading cycles until the crack initiation and the number of loading cycles until the complete failure is introduced next.

The corresponding analysis leads to the following dependence:

$$N_e = \frac{15.625 \cdot \eta_N}{(\eta_N - 1)^3} \tag{9}$$

Table 2 shows the values of η_N as a function of N_e. For N_e between 10 and 30, the durability factor margins η_N can be reduced from 4 down to 2.5 to 2.0.

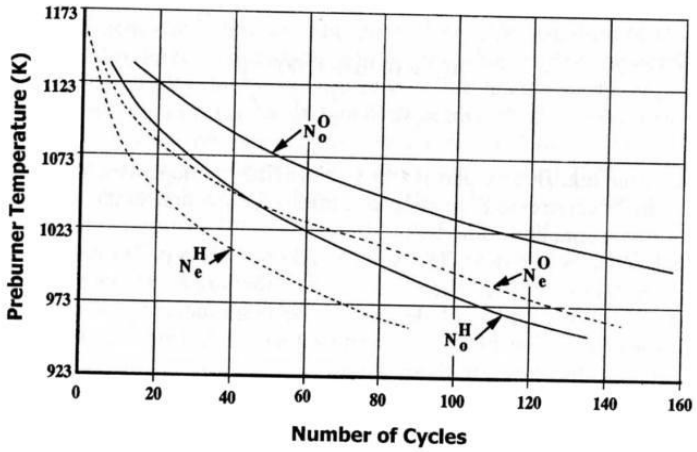

Fig. 3 Number of cycles to crack initiation (N_o) and operational cycles (N_e) as functions of preburner gas temperature and fuel-rich (H) and oxidizer-rich (O) turbine drive gas.

Table 2 Comparison of durability margin factor and number of loading cycles (or engine starts)

η_N	6.0	4.0	3.0	2.5	2.0	1.8	1.5
N_e	~1.0	~2.0	~6	~12	~31	~55	~187

With these concepts defined, the allowable values of operational use of the engine depending on the preburner gas temperature can now be analyzed. The dependence of preburner gas temperature T_g on N_e was shown on Fig. 3. The maximum allowable preburner gas temperature in the oxidizer-rich scheme for an engine with 25 starts is 1075 K, where no account was made toward the possibility of burning of the metal.

When the fuel-rich scheme in the tripropellant engine with tripropellant or bipropellant preburner is used, the preburner gas contains hydrogen, which can cause a reduction of the strength properties of the turbine blade material because of the problem of hydrogen embrittlement. The level of embrittlement is known to depend on the temperature, pressure, and the combination of gases present including hydrogen. High hydrogen pressure in lines and turbopump assemblies does not necessarily lead to problems with hydrogen embrittlement. In preburner gas lines, although the hazard of hydrogen embrittlement is present, the effect of hydrogen embrittlement is reduced because of both the high temperatures and the presence and influence of other components in the gas (such as water vapor). Engine design and manufacture procedures can account for the reduction of the plastic properties of the materials because of hydrogen embrittlement, since the extent of the plastic properties reduction is known.

During engine operation in flight, the temperature of the turbine blades changes from ambient temperature to the maximum during startup, and from maximum to ambient temperature during shutdown. To estimate the durability, material strength properties of the blades over the whole range of temperatures are required, taking into account the influence of embrittlement. For the tripropellant engine that transfers operational modes during flight from tripropellant to bipropellant, the hydrogen environment has influence on both modes of the engine operation.

Using the same concepts of the estimation of the durability of turbine blades operating in environments containing hydrogen, for 25 engine starts the allowable maximum preburner gas temperature is calculated to be 1033 K.

After calculation of the maximum allowable preburner gas temperature for the reusable engine, the nominal gas temperature can be calculated. From the maximum preburner gas temperature are subtracted the possible temperature changes ΔT that are connected with changes of external factors (variations of inlet pressures and temperatures of hydrogen, kerosene, and oxygen), changes of internal factors (variations of pump efficiencies, pump heads $H = \Delta p/\rho$), hydraulic characteristics of the units, and changes of the engine operational modes concerning the thrust and mixture ratio. In this case the nominal

temperature of the preburner gas can be estimated by

$$T_{g,\text{nom}} = T_{g,\max} - \Delta T_{\text{ext}} - \Delta T_{\text{int}} - \Delta T_F - \Delta T_{r_m} \tag{10}$$

where

$T_{g,\max}$ = maximum allowable temperature of preburner gas,
ΔT_{ext} = temperature variations caused by inlet conditions variations,
ΔT_{int} = temperature variations caused by engine-to-engine variability,
ΔT_F = temperature variations caused by changes of thrust F,
ΔT_{r_m} = temperature variations caused by changes of mixture ratio r_m.

The calculations of the preburner gas temperature variations in each group can be made to take into account the occasional and systematic laws of changes of these influencing factors. An engine designer must decide according to the technical requirements and the technology of the unit fabrication, especially important for such units as turbopump assemblies, what kind of occasional or systematic laws to use to take this into account. At the present time, the technical requirements for the tripropellant and multi-usable full-scale engine are not yet defined. An estimate of the nominal preburner gas temperature can be made based on temperature uncertainties ΔT_i from RD-0120 engine experience, for which the total sum of the possible preburner gas temperature variations is 149 K.

Using that estimation for the variations, the maximum allowable nominal preburner gas temperature for the fuel-rich scheme is $T_{g,\text{nom}} = 884$ K, and for the oxidizer-rich scheme is $T_{g,\text{nom}} = 926$ K. This difference is less than 5%, which is not significant when choosing the preburner gas combination for development of the tripropellant engine.

D. Soot Formation in Fuel-Rich Preburner

One problem associated with a fuel-rich hydrocarbon preburner is the possibility of creating solid carbon condensate, or soot, in the combustion products. Soot is a common byproduct in the turbine drive gas produced by fuel-rich oxygen/kerosene gas generators used in expendable open-cycle liquid rocket engines.[35] In simplest form, the predominant chemical reaction that creates soot in hydrocarbon reactions with oxygen is the recombination of carbon monoxide, CO, as follows:

$$2\text{CO} = \text{CO}_2 + \text{C}_s \tag{11}$$

where C_s is solid carbon, or soot. This is a non-equilibrium process not related to the total amount of CO, but it is a strong function of combustion gas pressure and temperature.

To avoid excessive component replacement or maintenance to remove soot from the internal passages of a reusable engine, the production of soot in the preburner must be minimized or eliminated. Preliminary analytical and experimental research in Russia suggested that organizing the burning processes in the tripropellant preburner with the correct application of propellant properties, injection distribution, and gas constituents precluded the possibility of soot formation. The addition of hydrogen to the fuel-rich, sooting hydrocarbon reaction with

oxygen changes the amount of soot in two ways: 1) by eliminating the soot by reacting with it to create methane, CH_4,

$$\text{C}_s + 2\text{H}_2 = \text{CH}_4 \tag{12}$$

and 2) by precluding its creation by reacting with the CO,

$$2\text{CO} + 2\text{H}_2 = \text{CO}_2 + \text{CH}_4 \tag{13}$$

However, because the injection and mixing schemes in full-scale designs are dependent on size and can considerably influence the processes of combustion, more development experimentation was required to demonstrate soot-free operation. The design task was additionally complicated by the requirement for the preburner to satisfactorily operate in both tripropellant and bipropellant modes with fixed hardware geometry, and to transition without problems from one mode to the other.

For these reasons, single-element and multi-element preburners (called models in Russia) were developed for testing various preburner mixing schemes and injection element designs prior to testing in the full-scale preburner.[36,37] These model preburners used the same injection element geometries and propellants as in the full-scale preburner, but in reduced-size combustion chamber hardware. Two variants of mixing schemes—a one-zone process and a two-zone process—were tested in the model hardware using different variants of injection elements. In the one-zone mixing process, all the propellants were injected at the head end of the chamber, while in the two-zone mixing process, the hydrogen was injected at a downstream location.

The primary objectives of the model hot-fire tests were to 1) choose the optimum mixing scheme and injection element for soot-free tripropellant operation, 2) verify the capability to sample and measure the composition of the combustion products (including soot, if present), 3) examine the nonuniformity of the combustion gas temperature field, and 4) investigate the conditions of ignition, providing for startup and shutdown transients without temperature excursions or soot generation. Additional objectives from the unique requirements of dual-mode tripropellant engine operation included: 1) transition from tripropellant to bipropellant operation without soot generation or temperature and pressure excursions, 2) operate in bipropellant mode with minimum temperature nonuniformity, and 3) shutdown in bipropellant mode without temperature excursions.

1. *Model Preburner Testing*

Four variants of injection elements in each of the one-zone and two-zone mixing schemes were tested in single-element and eight-element model tripropellant preburners.[36,37] Chamber pressures ranged up to 13 MPa, and test durations were typically 20 s.

Test conditions were selected to provide operational modes of the preburner for the standard tripropellant engine flow splits (6% hydrogen, 12.6% kerosene, and 81.4% oxygen). Test conditions also included varying the overall mixture

ratio over a wide range, $r_g = 0.20-0.90$, and varying hydrogen-to-kerosene ratios at the same overall mixture ratio r_g.

To evaluate the combustion process in the preburners and verify soot-free operation, the gas composition and soot concentration were sampled during hot-fire testing. The gas sampling system is described in detail in Ref. 36. It was designed to discourage further reactions among chemically active components after sampling, and to avoid distorting the phase composition (i.e., soot) of the sampled gas. The sampled gas was initially cooled in a water-cooled sample probe, and then further cooled to 10–20°C in a water-cooled heat exchanger until it reached chemical equilibrium. The sampled products were then directed into a centrifugal separator where soot fell to the bottom of a sample cup. After a test, this cup was weighed and compared to the weight before the test to determine soot quantity collected in the cup during the sample time.

In a different version of the sample gas system, the centrifugal separator was removed and the gas directed through a filter to measure soot quantity. The filter was made from titanium powder by powder metallurgy and had a filter rating equal to 10 μm and a thickness of 3–4 mm, with the labyrinth cross section of the filter capable of capturing soot. Pressure sensors were installed in the line to monitor pressure drop across the filter. With no soot in the sample gas, the pressure drop across the filter remained constant. During an operational mode where soot was present, the pressure drop across the filter began to increase, indicating that the filter was being contaminated and filling with solid matter. The intensity of this filling provided a means to determine exactly when sooting was occurring in the preburner chamber, and how strongly. When the operational mode initially began to change to one where sooting occurred, the pressure drop across the filter slowly increased, but when the mode was completely achieved, the pressure drop increased intensely, indicating the presence of soot. With this method, the time and conditions of soot appearance were clearly established. The filters were also weighed before and after the test, with the net weight increase attributed to soot in the gas stream.

The presence of soot in the model testing was thus determined by three quantitative techniques: 1) mass change in the sample cup and filter in the gas sample system, 2) increase in pressure drop across the filter in the gas sample system, and 3) differences between measured and predicted equilibrium combustion gas temperature and pressure. Soot was also shown qualitatively by review of video of the exhaust plume, where a transparent exhaust was a verification of soot-free operation.

According to mass changes of the sample cup and the filter, the combustion gas at nominal operating modes produced only trace amounts of soot. At conditions outside the range of normal operation, near the boundaries where soot began to occur, measured soot content in the combustion gas, given in percent of the total mass of the combustion products gas, ranged from 1 to 4%. No measurements were attempted where severe sooting occurred. These measurements clearly defined the operating conditions required for soot formation and determined the boundaries for soot-free operation. Analyses of these test data showed that operation of the preburner in nominal tripropellant mode without soot formation was possible up to a chamber pressure of 50 MPa.

The absence of soot was also verified, in addition to sampling the combustion products, by comparing measured preburner chamber pressure p_e with calculated pressure p_p, and measured preburner gas temperature T_e with calculated temperature T_p. The comparison between experimental and analytical chamber pressures in the preburner is one way to determine the completeness of combustion and whether soot has been generated in the preburner combustion gas. Calculated pressure was determined using the measured gas temperature, propellant flow rates, and the results of the combustion product composition analyses. If the experimental pressure was less than the calculated value ($p_e < p_p$), then either some of the preburner products did not participate in creating pressure in the preburner chamber (i.e., soot exists) or the combustion was incomplete. Under nominal tripropellant operating conditions as previously defined, high efficiencies of combustion were obtained, with measured pressure 95–100% of calculated pressure, suggesting combustion was mostly complete and soot was not present. However, a drastic reduction in efficiency (less than 85%) was observed during portions of tests where sooting was suspected, suggesting that soot was present at those moments, which agreed with the measurements of soot made in the gas sample systems. Comparison of experimental and analytical preburner chamber pressures showed that, to operate without generating soot in the preburner products, increasing the overall mixture ratio r_m was required.

The uniformity of the combustion gas temperature field is an indication of the mixing level in the injection design, which can also influence the creation of soot at local levels. For all tests conducted, the temperature field was measured by thermocouple rakes at two circumferential locations. Each rake contained either four or eight thermocouples located radially at even intervals along the rake lengths. The maximum temperature non-uniformity did not exceed $+8/-30$°C at average T_e of 700–750 K. This is a high level of uniformity ($+1/-4$%), indicating a satisfactory injection process design for preburner development.

The results of the model preburner tests showed that the basis for development of a soot-free kerosene/hydrogen/oxygen preburner was correct, and that operating without soot was possible over a satisfactory range of operating conditions necessary for power generation in the tripropellant engine.

2. *Full-Scale Preburner Testing*

Following model testing, a one-zone full-scale preburner was fabricated and tested. A cross-sectional detail of this preburner is shown in Fig. 4. The one-zone mixing scheme, with all propellants injected at the head end of the chamber, simplified the design and fabrication. The injection element chosen for the full-scale preburner, based on results of the model testing, is shown in Fig. 5. The element includes oxidizer swirl and both swirled and angled kerosene injection. Hydrogen is injected from the faceplate. Additional kerosene orifices, as shown in Fig. 4, were included on the injector face to provide for the balance of kerosene injection area.

For full-scale preburner testing, a test bench was constructed that included an assemblage of valves and pipes exactly as would appear on the tripropellant engine. With such a configuration, the start transient, mode transfer, and shut-

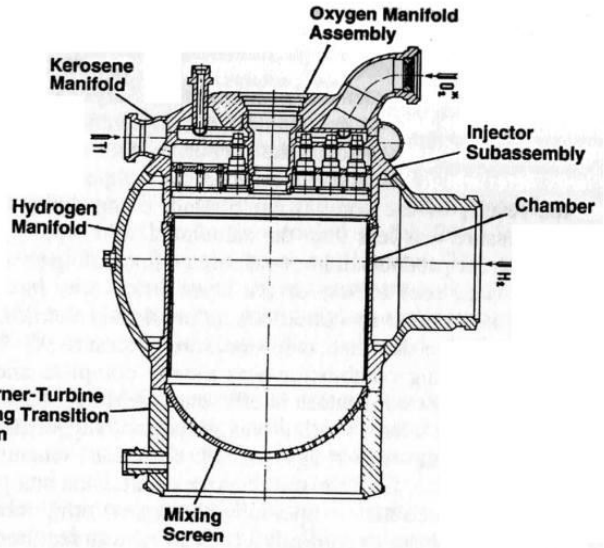

Fig. 4 Cross-section of one-zone full-scale tripropellant preburner.

down transient of the preburner can be examined and developed in a much more realistic fashion. An orifice simulating the turbine and main chamber resistance was installed at the preburner chamber outlet.

Five tests of the full-scale preburner were conducted and were reported in Ref. 37. During tripropellant operation, no soot was detected in the sampled gas by filter pressure drop or filter weight change, or in the exhaust plume by examination with video. Although the preburner was tested at low chamber pressures—to the limits of the test stand—predicted pressures matched model

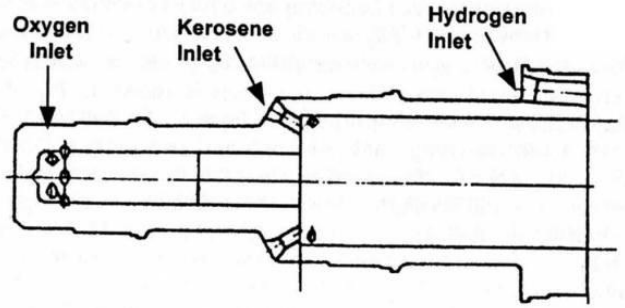

Fig. 5 Cross-section of injection element used in one-zone full-scale tripropellant preburner.

preburner test data, indicating soot-free operation is expected at higher pressures by similarity to the model data.

The temperature fields of the preburner chamber for bipropellant and tripropellant modes were evaluated using two seven-thermocouple rakes. The maximum temperature nonuniformity for the tripropellant mode, including the low temperature at the boundary layer near the wall, ranged from +48 to −40 K for a total temperature differential of 88 K based on a mean temperature of 833 K, or $\pm\sim5\%$. The maximum temperature nonuniformity for the bipropellant mode, including the low temperature at the boundary layer near the wall, ranged from +43 to −46 K for a total temperature differential of 89 K based on a mean temperature of 850 K, or $\pm\sim5\%$. At these low-power operating levels, both of these temperature nonuniformities were acceptable.

The operational stability was evaluated based on the pressure oscillations measured in the fuel and oxidizer manifolds. Low-frequency pressure oscillations were completely absent during the bipropellant mode, while operating at about 25% of nominal power. During the tripropellant mode, there were low-frequency pressure oscillations between 40Hz and 60 Hz with amplitudes reaching about 9–12% of the nominal preburner chamber pressure in the oxidizer manifold and about 4–7% of the nominal chamber pressure in the fuel manifold. These oxidizer manifold oscillations were mild and did not influence the preburner gas temperature or temperature uniformity, so that the preburner operation was still considered stable. The oscillations were caused by operating at a tripropellant preburner chamber pressure of only about 10% of nominal. At this chamber pressure, the injection element pressure drops were very low (less than 2% of preburner chamber pressure).

Within the limits of the test stand capability, the full-scale preburner was found to operate without soot and with acceptable thermal and stability variations. Comparison with the model testing showed that the full-scale preburner should operate satisfactorily at higher chamber pressures.

III. Tripropellant Engine Using Fuel-Rich Closed-Power Cycle

A. Optimum Engine Schematic

The schematic of the optimum closed-cycle tripropellant engine with a tripropellant fuel-rich preburner is shown in Fig. 6. The operating and design parameters of this engine at a main chamber pressure of 24.5 MPa are listed in Table 3, which were calculated for a propellant combination consisting of 6% liquid hydrogen, 12.6% kerosene, and 81.4% liquid oxygen, and an overall $r_m = 4.376$. The vacuum thrust and specific impulse were calculated with an exit nozzle diameter of 2300 mm and geometrical expansion ratio of 104.5 : 1.

This engine contains three groups of turbopumps: 1) booster and main liquid oxygen pumps with gas turbines, 2) booster and main liquid hydrogen pumps with gas turbines, and 3) liquid hydrogen kick pump and main kerosene pump with gas turbine, which are on the same axle, and the booster kerosene pump with gas turbine. The use of two hydrogen pumps is a peculiarity of the engine due to the dual-mode operation. The hydrogen flow rates for tripropellant mode and bipropellant mode are practically equal, as shown in Table 3, but the discharge pressure after the main hydrogen pump drops 2 or 2.5 times in the

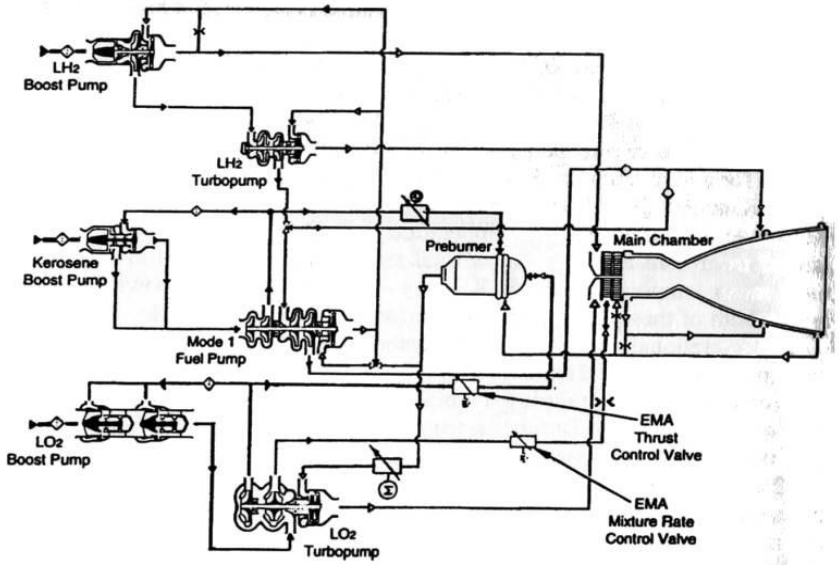

Fig. 6 Schematic of optimum closed-cycle tripropellant engine with fuel-rich turbine drive.

bipropellant mode. Such a range requires two hydrogen pumps for tripropellant mode and one pump for bipropellant mode. One hydrogen pump (along with the kerosene pump) is switched off during transition from tripropellant to bipropellant mode.

To adjust and control the engine operational modes, there are four controlling valves: 1) the liquid oxygen regulator in the preburner feed supply duct, for control of thrust, 2) the kerosene regulator in the preburner feed supply duct, 3) the gas throttle in the hot gas duct between the main liquid oxygen turbopump turbine and the main liquid hydrogen turbopump turbine, and 4) the liquid oxygen throttle in the main injector feed duct, for control of mixture ratio.

One unique feature of this tripropellant engine scheme is that all of the hydrogen flow is supplied to the combustion chamber for chamber wall cooling. The use of heat resistant coatings on the hot copper wall of the chamber is not considered because of the requirements that the tripropellant engine be reusable. The use of different coatings can reduce the reliability because these coatings may not be adequately bonded to the metal chamber walls. Therefore, to maintain a nominal hot-gas copper wall temperature at 800 K, provision of a cold film near the wall is required to reduce the heat transfer to the chamber wall. Because of its superior cooling capabilities, hydrogen can cool the copper chamber wall with a specific heat flux of $90-100 \times 10^6$ kcal/(m^2 · h), and with acceptable hydraulic losses in the cooling ducts assuming coolant flow speed of 250–300 m/s. When the chamber pressure is increased, the specific heat flux also increases, and to reduce the heat flux to allowable values, the mixture ratio in

Table 3 Main parameters of optimum fuel-rich tripropellant engine for reusable vehicle with 25 cycles between refurbishments

Parameter	Units	Tripropellant	Bipropellant
Propellant combination	——	6.0% H_2, 12.6% K, 81.4% O_2	14.3% H_2, 85.7% O
Vacuum thrust	mT	200	80
Sea-level thrust	mT	157.1	——
Sea-level thrust with insert	mT	171.2	——
Vacuum specific impulse	s	409.1	454.0
Sea-level specific impulse	s	321.3	——
Sea-level specific impulse with insert	s	350.2	——
Main chamber pressure	MPa	24.5	10.3
Overall mixture ratio	——	4.376	6.0
Total propellant flow rate	kg/s	488.9	176.2
Liquid oxygen flow rate	kg/s	398	151
Liquid hydrogen flow rate	kg/s	29.3	25.2
Kerosene flow rate	kg/s	61.6	——
Preburner gas temperature	K	850	815
Preburner gas constant	$\frac{kg_f - m}{kg - K}$	122.5	280
Preburner mixture ratio	——	0.581	0.515
Preburner total propellant flow rate	kg/s	143.7	38.2
Preburner liquid oxygen flow rate	kg/s	52.8	13.0
Preburner liquid hydrogen flow rate	kg/s	29.3	25.2
Preburner kerosene flow rate	kg/s	6.6	——
Nozzle expansion ratio	——	32 : 1	104.5 : 1
Nozzle exit diameter	mm	1400	2300

the film by the hot gas wall must also be reduced, which causes a reduction of the specific impulse of thrust. Figure 7 shows the change of the mixture ratio of the combustion products in the wall boundary-layer film with changes in chamber pressure according to 1) an expendable chamber with nickel-chrome heat resistant coating on the combustion chamber wall, where the number of thermal cycles (start plus stop) is 5 or less, and 2) a reusable chamber where the number of thermal cycles is 25. Then, based on these dependences, the vacuum specific thrust impulse with a fixed nozzle exit diameter equal to 2300 mm (or a fixed engine envelope) with different chamber pressure can be calculated, as shown on Fig. 8. Thus, for expendable combustion chambers, the optimum vacuum specific impulse occurs with a chamber pressure of about 34.5 MPa, while for reusable combustion chambers the optimum occurs at a chamber pressure not higher than 24.5 MPa.

As a rule, the hydrogen is first supplied to the throat section to provide reliable cooling of this critical section, and then through the chamber to the

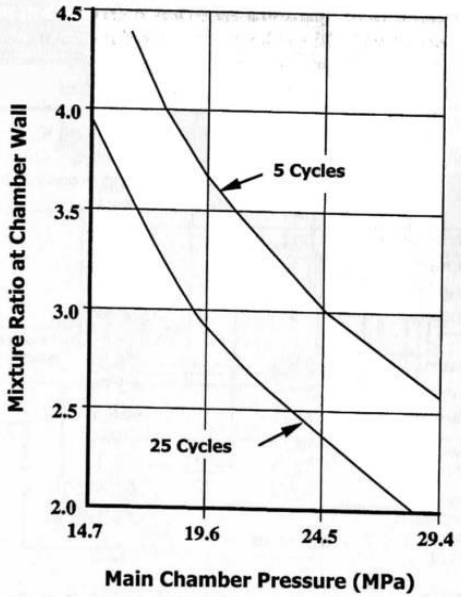

Fig. 7 Effect of number of operating cycles and main chamber pressure on the mixture ratio required at main combustion chamber wall.

head end, and finally in a series path through the nozzle. To decrease the overall hydraulic resistance of the cooling duct flow path, the nozzle can also be cooled by oxygen flow, due to the low level of the specific heat flux in that region, although that is not used on the current schematic. The coolant supply of oxygen is then mixed with the rest of the oxygen, which then proceeds to the main injector.

B. Engine Characteristics with Dual-Mode Operation

1. Main Injector Performance

For the tripropellant engine shown in Fig. 6, the mixing elements in the main injector operate with gaseous and liquid fluid states in both modes. Consequently, the development of the mixing elements and the combustion chamber head of existing O_2/H_2 staged combustion engines (such as the RD-0120 engine) can be used for design of the main injector for the tripropellant engine.

Results of uni-element mixing and combustion process experiments conducted during the development of the RD-0120 engine main injector are shown in Fig. 9. The experimental dependence is shown between completeness of combustion in the combustion chamber for coaxial atomization injector elements operating with fuel-rich preburner gas and liquid oxygen, and the

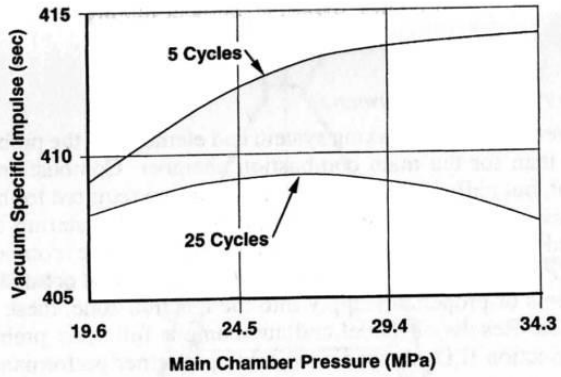

Fig. 8 Effect of main chamber pressure and number of operational cycles on vacuum specific impulse.

ratio of gas injection momentum to liquid oxygen injection momentum. Increasing this momentum ratio clearly increases the efficiency of combustion of the propellants in the chamber. The data shown in Fig. 9 provide a means to analyze the potential performance of these mixing injector elements when operating in tripropellant and bipropellant modes. The momentum ratio for the injector element in the tripropellant mode (i.e., with tripropellant fuel-rich gas for fuel) is about 0.3, and the combustion efficiency is higher than 0.995. The momentum ratio for the injector element in the bipropellant mode (i.e., with bipropellant fuel-rich gas for fuel) is about 0.2, so that the combustion efficiency of the elements would

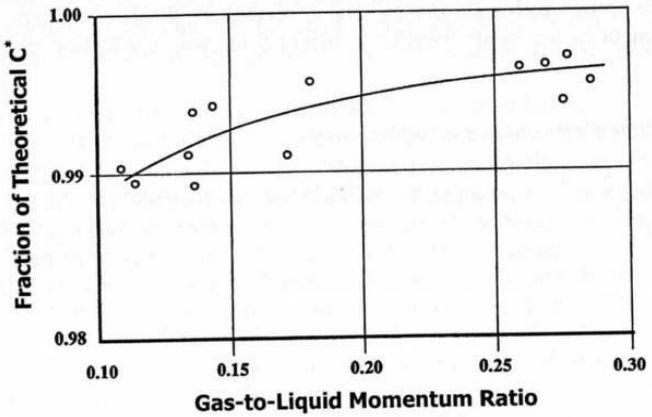

Fig. 9 Characteristic velocity efficiency of RD-0120 injection elements as function of gas-to-liquid element momentum ratio—single-element hot-fire data.

be about 0.995. For both modes, then, the element mixing performance remains high.

2. *Preburner Injector Performance*

The requirements for the mixing system and elements of the preburner injector are different than for the main combustion chamber. Combustion efficiency is less important, but uniform gas temperature fields are required for both operating cases, and there can be no temperature spikes during the startup and shutdown transients and the mode transfer transient. Because the combustion of the propellants for tripropellant and bipropellant modes can be organized with independent systems of propellant supply into the reaction zone, these requirements can be satisfied. Results of model and autonomous full-scale preburner testing, presented in Section II.D, showed acceptable preburner performance.

3. *Mode Transfer Transients*

During the transition of operation of the engine from the tripropellant to bipropellant mode, the kerosene pump and the high-pressure hydrogen pump are turned off. Because the three propellants are supplied independently to the preburner (with the oxygen as a cryogenic liquid, the kerosene as a room temperature liquid, and the hydrogen as a room temperature gas), during the transition between modes the kerosene manifold must be filled with hydrogen. This operation does not freeze the kerosene, because the hydrogen supplied to the preburner is at room temperature. However, for proper timing, the hydraulic resistance of the hydrogen and kerosene feed ducts must be considered for both tripropellant and bipropellant conditions. During the process of switching modes, liquid kerosene and warm hydrogen are mixed together in the preburner kerosene line for some time, until the kerosene pump is turned off. During this time, the engine control system switches all engine systems over to bipropellant mode operation. Satisfactory mode transfer operation was demonstrated in testing of the model and autonomous full-scale preburners, described in detail elsewhere.[36,37] Final development of the mode transfer transient must wait for testing in a complete engine.

4. *Altitude Performance Compensation*

RLVs require a combination of high sea-level takeoff thrust and high vacuum specific impulse performance. To increase both with an SSTO vehicle, some type of altitude compensation in the engine is necessary to provide the required mission-average performance. Modifications of the supersonic portion of the standard bell nozzle are required. One simple variant under development provides an insert in the supersonic portion of the nozzle, as shown in Fig. 10, that is removed at some appropriate moment in flight.[38]

The ejectable insert involves fixing a carbon-carbon insert in the nozzle to reduce the expansion ratio at low altitudes and prevent separation of the exhaust plume. At the appropriate time in the trajectory, the insert is released and guided cleanly out of the nozzle, increasing the expansion ratio for efficient high-altitude operation. The insert is made of carbon-carbon composite material

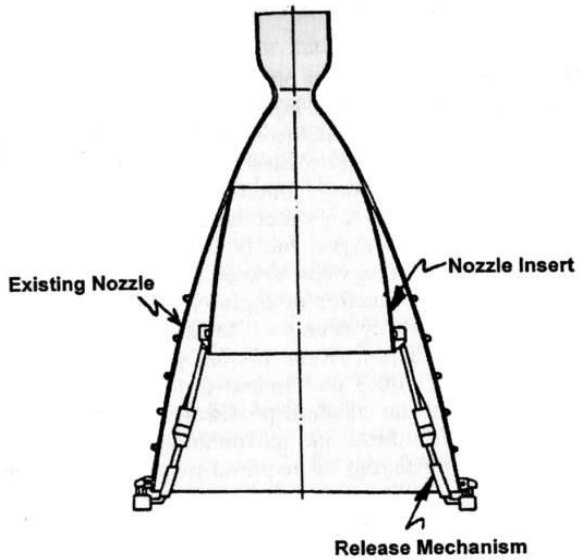

Fig. 10 Altitude compensating nozzle insert for tripropellant engine with single bell nozzle.

to minimize weight and eliminate the necessity for active cooling, and has a profiled contour to provide the highest performance characteristics. The insert is constructed to reduce the geometrical area of the nozzle extension, as shown in Fig. 10, and hence eliminate the appearance of shock waves during the startup and shutdown transients. Consequently, the vibration loads on the nozzle structure are decreased. The geometrical dimensions of the insert and the moment when it is removed are defined by the gas dynamic characteristics of the combustion products flows and by the performance requirements of the rocket flight trajectory.

Full-scale hot-fire experiments with the RD-0120 engine have been conducted with the ejectable insert and have demonstrated the durability of materials, seals, and release mechanisms with gas temperature equal or less than 2200 K.[38] With one of the variants of the inserts installed in the nozzle, the sea-level specific thrust impulse in a 50% operational thrust mode increased by 21.8%, providing for a prediction of an increase of sea-level specific thrust impulse of 9.2% at the 100% operational thrust mode.[38] Vibration levels at sea level were decreased by 16–36 G^2/HZ.[38]

The use of an insert for altitude compensation has several advantages. No changes to an existing nozzle are required to use the insert for altitude compensation. Because the insert is a separate, bolt-on component, adaptations are easily made to re-optimize specific parameters for other missions. The low replacement costs, short fabrication lead times, and three-hour replacement time are very compatible with scenarios for reusable vehicles.

C. Requirements for Reusability and Operability

1. RLV Engine Life Improvements

A key factor in making an RLV cost effective is the ability to amortize the purchase price of high-cost items, such as liquid rocket engines, over a large number of uses. Consequently, increasing the life of the liquid rocket engines is critical. A life prediction methodology that relates engine durability (operating cycles and duration) to engine operating conditions has been developed.[34] This methodology is based primarily on structural analysis techniques, accounting for both low and high cycle fatigue, but is also anchored to test data of the RD-0120 engine. The methodology can be used to analyze specific design modifications, predicting life as a function of engine operating parameters.

The methodology has already been used to assess increasing the life of the existing RD-0120 engine. The Energia mission profile required that the RD-0120 operate primarily at 106% of nominal thrust. The engine qualification program demonstrated that the standard production configuration under simultaneous conditions of 106% thrust and maximum mixture ratio can deliver six hot-fire cycles, without infringing on required margins or affecting the 0.992 reliability. The life-limiting feature demonstrated by the engine in serial production configuration was the appearance of cracks in the trailing edges of the turbine blades on the main turbopump. Implementing an identified modification to the turbine blades and the shroud is predicted to increase life by an order of magnitude.[34] Further identified design modifications on the next life-limiting features, such as main combustion chamber and main turbine nozzle cracks, will increase the life limit of the engine further.[38] The effects of these changes on the predicted existing RD-0120 engine life are shown in Fig. 11.[34,38] Such improvements as already identified on an existing engine strongly support that RLV life requirements can be achieved on the tripropellant engine as well.

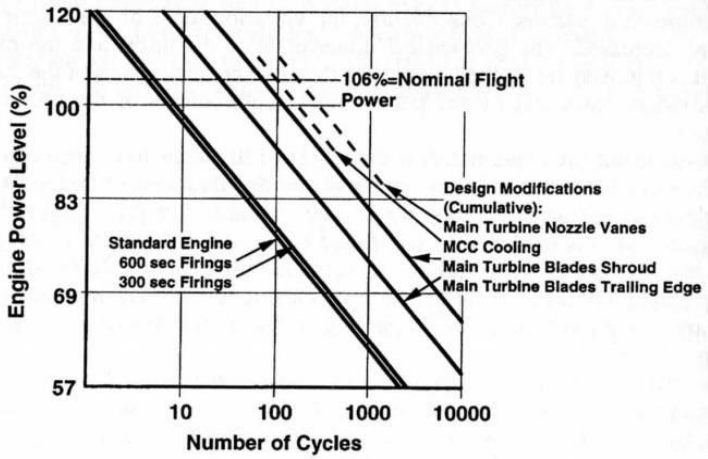

Fig. 11 Improvements in flight RD-0120 engine life due to identified engine modifications.

2. RLV Operability Issues

Labor, equipment, and facilities for initial launch preparation and recycling between flights are a major factor in the life-cycle cost of any reusable vehicle. Quick, low-cost ground operations are absolutely essential to a cost-effective SSTO RLV and will determine the economic feasibility of the concept.

The Russian approach to operations has always emphasized rapid launch preparations with minimal equipment and simple procedures.[38] The RD-0120 engine had the advantage of a legacy of dozens of previous engine developments and thousands of flights that have refined this basic approach. The design of the engine system and the designs of individual components incorporated lessons learned in automated checkout, elimination of maintenance, tolerance of extreme conditions, and management of conditions, such as leakage, which are difficult and costly to completely eliminate. RD-0120 engine operations have been well characterized in the course of preparation for approximately a thousand engine firings (for both ground and flight tests).

A test program was conducted with emphasis on measuring the operability parameters of the RD-0120 engine.[39] Service time on the engine of 48–72 hours and 250 manhours was all that was required to return the engines to test.[39] These are representative numbers desired for RLV operation.[38]

3. Weight Reduction

High thrust-to-weight at sea level is an absolutely essential feature for the RLV main engine. The nozzle program discussed in Section III.B is a large contributor toward reaching an RLV weight requirement, a synergistic effect of the higher sea-level thrust available from the altitude compensating design and of the lower weight.

Additional weight reductions are necessary, however, and a review of the existing RD-0120 engine, for example, shows that some easily implemented solutions are available. These include changes in the size, configuration, and materials of the propellant inlet ducts. Inlet ducts are relatively massive, and modifications offer the possibility of significant improvements without disturbing the arrangement or functioning of the engine. Removal of external insulation on hot and cold ducts is another relatively high payoff modification. More intrusive weight reductions for the RD-0120 engine require longer-term solutions, such as shifting to higher-strength materials for certain components.[38]

4. Controls and Health Monitoring

For a reliable and reusable vehicle, health monitoring and properly responsive control systems of the engines are important aspects of operability. The assessment of engine health during ignition and flight and the correct response to problems will be critical to avoid sacrificing payloads. The level of development required may not be as large as may appear, however. Sophisticated and effective control laws and safety system algorithms have already been developed and proven for the RD-0120 engine for operation on the Energia vehicle,[33] and their effectiveness is shown by the high demonstrated reliability. One important new requirement is that the control system be autonomous. Engine control system

autonomy permits independent development of the vehicle systems and avoids conflicting schedules, requirements, and priorities. With software programmability, operating modes can be rapidly reconfigured and optimized to reduce development testing and operational timelines. Functional redundancy, automated checkout, and integrated condition monitoring and problem diagnosis will improve reliability and reduce life cycle costs.

IV. Use of RD-0120 Engine for Development of Tripropellant Engine

The development cost of a rocket engine, especially for booster applications, is a substantial investment and can be prohibitive. This cost can redefine features of the design or be the ultimate deciding factor between paper and reality. Consequently, the use of previously developed and qualified engines and components is a great advantage that can save money and make new or "next-generation" designs feasible. Because of significant similarities to the RD-0120 engine, as suggested by previous sections of this chapter, a fuel-rich tripropellant engine can use this evolved approach for development.

Tripropellant engine development issues that could be considered already developed because of the design, fabrication, and test history of the RD-0120 engine include: 1) achieving highly efficient combustion processes in the main combustion chamber with injection of liquid/gas cryogenic propellants, 2) development of transpiration cooling of the main chamber injector face, 3) development of the main chamber cooling techniques, 4) creation of a milled, jointless supersonic nozzle with large dimensions, 5) use of powder metallurgical technology for fabrication of turbine blades, 6) creation of efficient axial unloading in the turbopump unit, 7) development of high-frequency rotor balancing methodology for the turbopumps, 8) selection and development of the experimental materials in regard to the hydrogen influence on their mechanical strength properties, 9) design of the units and engine overhaul concerning reusability and long life of operation, and 10) creation of the safety system and monitoring the technical state of the engine after hot-fire tests.[33]

Engine development problems solved during the design, fabrication, and test of the RD-0120 engine whose solutions could be used for tripropellant engine development include: 1) achieving uniform temperature distributions in the preburner with injection of cryogenic propellants, 2) development of engine startup and shutdown transients, and 3) creation of the system to control the engine modes.[33]

Obviously, many of the most difficult technical issues of the fuel-rich tripropellant engine development have already been solved. In addition, the methods of development and experimental verification that were previously developed can be used during the development of the tripropellant engine.

For these reasons, the RD-0120 engine can be used to provide a rapidly integrated and low-cost technology demonstration of a tripropellant kerosene-hydrogen-oxygen engine with a fuel-rich turbine drive.[38,40] Most of the existing bipropellant engine hardware can be incorporated directly into the tripropellant engine demonstration, with no changes whatsoever to approximately 95% of the flight-qualified component designs. A comparison of the bipropellant RD-0120 engine and a tripropellant engine demonstration, shown in Fig. 12,

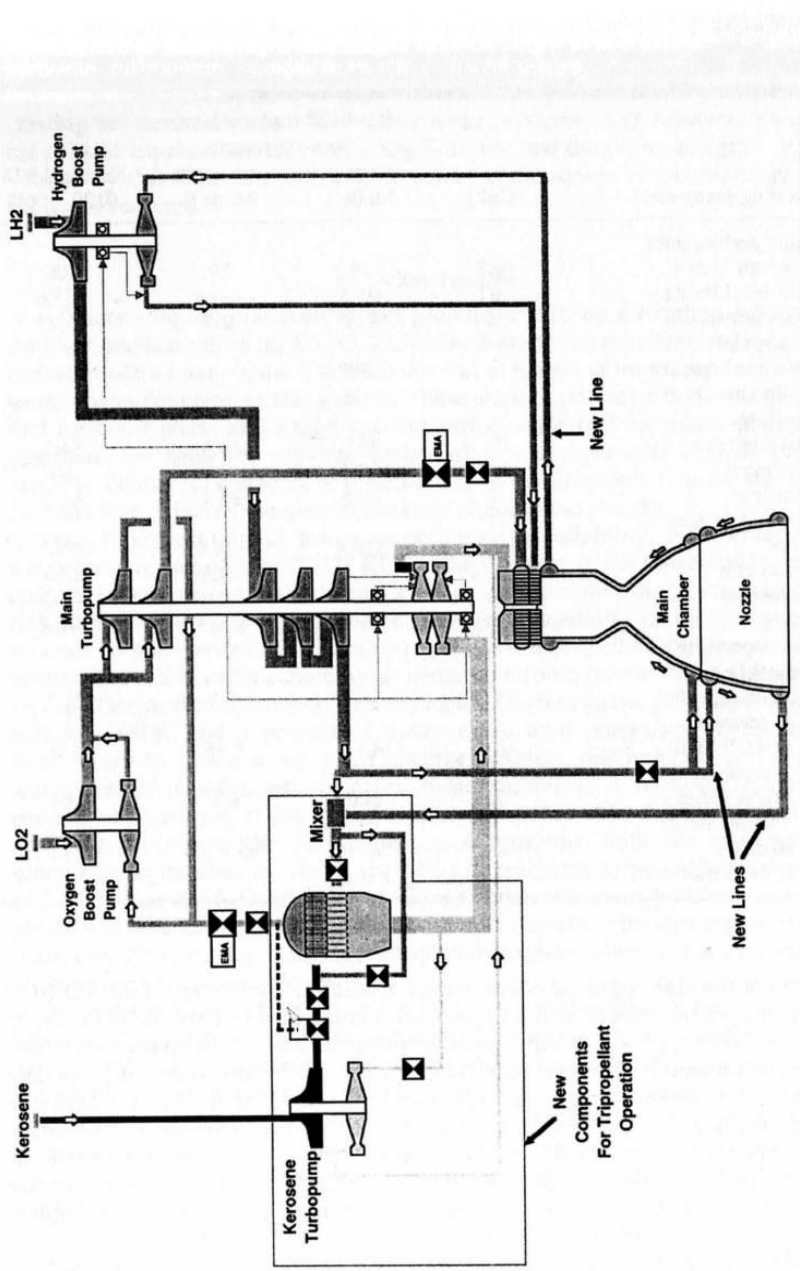

Fig. 12 Comparison of flight RD-0120 engine schematic and tripropellant demonstration engine based on RD-0120 engine.

Table 4 Comparison of flight RD-0120 engine and tripropellant demonstration engine based on RD-0120 engine

Operating parameters	Units	RD-0120 tripropellant demonstrator		Standard RD-0120, 106%
		Mode 1	Mode 2	
Engine performance				
Vacuum thrust	mT	134.3	79	200
Sea-level thrust	mT	94.5	——	155.6
Vacuum specific impulse	s	419	452	455.5
Sea-level specific impulse	s	295	——	354.0
Propellants				
Hydrogen	%	9.1	14.6	14.3
Kerosene	%	10.4	——	——
Oxygen	%	80.5	85.4	85.7
Propellant flow rates				
Total	kg/s	320.4	174.8	439.7
Hydrogen	kg/s	29.2	25.5	62.8
Kerosene	kg/s	33.2	——	——
Oxygen	kg/s	258.0	149.3	376.8
Engine operating parameters				
Main chamber pressure	MPa	14.7	8.1	21.9
Overall main mixture ratio	——	4.13	5.85	6.0
Preburner gas temperature	K	800	800	800
Nozzle expansion ratio	——	85.7 : 1	85.7 : 1	85.7 : 1

illustrates the high degree of commonality. Operating parameters of the RD-0120 and tripropellant demonstration engines are summarized in Table 4. The existing main turbopump, boost pumps, thrust chamber assembly, and most valves and lines can be used without changes. New components include only a tripropellant preburner, kerosene turbopump, and additional valves and lines for kerosene supply and kerosene turbopump turbine drive gas supply and exhaust. The tripropellant preburner, discussed in Section II.D, is itself an evolution of the RD-0120 design, incorporating modifications in the propellant manifolding and injector elements and adding a kerosene inlet, but retaining all the previous propellant inlet and structural interfaces.

Risk for the tripropellant engine demonstration can be minimized by an approach that emphasizes a step-by-step addition of capabilities. For the first step, the tripropellant preburner and associated control systems are installed, while kerosene is supplied by high-pressure facility tanks. Following

demonstration of operating characteristics and performance with this engine, a kerosene turbopump is added and a fully pump-fed tripropellant engine is demonstrated. Development of new turbomachinery is avoided by adapting an existing kerosene unit taken from other rocket systems. Any substantial technical risks of tripropellant engines, along with life and durability margins, can be verified by this demonstration engine before commitment to a completely new engine is required.

V. Conclusions

Advanced liquid propellant rocket propulsion will be a requirement for the eventual realization of an SSTO RLV. Dual-mode tripropellant engines have been considered both in the United States and in Russia as important competitive technologies for creating this vehicle. These engines provide a high bulk density fuel for boost phase and a high specific performance fuel for ascent phase, but eliminate the need for separate hydrocarbon and hydrogen engines on the vehicle. Vehicle dry weight is reduced due to smaller tank size for the boost fuel and less vehicle base area to package engines and nozzles.

One of the most critical factors for performance, reliability, and operability of a tripropellant engine in an SSTO RLV is the selection of the power cycle. In this chapter, the rationale for selection of a partial staged combustion cycle with fuel-rich turbine drive gas was presented. First, the capability of the drive gas to produce turbine power was examined. Fuel-rich tripropellant turbine drive gas possesses 6–58% more capability to generate turbine power than oxidizer-rich bipropellant turbine drive gas, over a range of turbine drive gas temperature of 850 to 1000 K, and a percent of hydrogen to total propellant in the engine from 4 to 6%. Because of thrust chamber cooling requirements and typical leakage rates in advanced hydrogen turbomachinery, it is unlikely that the percent of hydrogen in the engine will be less than 4%. For the propellants with 6% hydrogen, the preburner gas temperature with the oxidizer-rich scheme must increase by 200 K (or 14%) to reach the same chamber pressure of 24.5 MPa as the fuel-rich scheme. Conversely, at the same preburner gas temperature of 850 K, the fuel-rich scheme attains a chamber pressure approximately 5 MPa (or 25%) higher. These are substantial numbers when considering the life requirements for a reusable engine.

Second, the effects of the gas on the engine material reliability were discussed. Oxidizer-rich gas has the capability to ignite the metal ducting given unpredictable hazards as can happen in oxidizer turbines. Coatings on the exposed metals are not desirable for use on a highly reusable engine that would retain low operational costs. This type of ignition is not possible with fuel-rich systems. On the other hand, the problem of hydrogen embrittlement on metals is understood enough to be analyzed and avoided in the design of the structure, while providing the necessary reusability.

Third, analyses of the effects of the turbine drive gas on the turbine blades, which are currently the components with the least durability in these engines, showed that the maximum allowable fuel-rich turbine gas temperature to meet an engine life of 25 cycles between refurbishment was only 5% less than the turbine gas temperature of the oxidizer-rich gas, without discounting the metal

ignition hazard of the oxidizer-rich gas. This difference is much less significant at the required operating temperatures than the difference in turbine power.

Finally, few technical issues remain to be solved with this engine, mainly because of its similarity with other high-pressure, fuel-rich, staged combustion engines already developed and qualified. The most critical issue for fuel-rich tripropellant operation, sooting in the preburner, has been addressed. Soot-free fuel-rich tripropellant gas generation has been demonstrated in model and autonomous full-scale preburner testing. The tests showed that soot formation was precluded at preburner mixture ratios where soot would otherwise occur, and a sufficient soot-free operating range existed, so that sooting in the preburner would not limit engine operability. The model and full-scale preburner testing also successfully demonstrated the transient between tripropellant and bipropellant modes.

An optimal fuel-rich tripropellant engine scheme was presented. A review of this scheme suggests that issues about engine life, durability, and operability need to be addressed, along with perceived issues of excessive complexity and reduced reliability due to additional engine components with an additional propellant. However, because of the similarity to an existing engine, some of these issues can be assessed now. A life methodology has been developed and shows that the existing RD-0120 engine can reach the life required for RLV. Additionally, because of the Russian approach to operations, emphasizing rapid preparations, minimal equipment, and simple procedures, engine operability requirements are also at acceptable levels for RLV. For the other questions, an engine test demonstration is required. A demonstration tripropellant engine can be quickly brought to test using the RD-0120 engine as the basis. This demonstration would emphasize that the tripropellant engine would not be a new development but an evolution from an existing, flight-qualified engine—probably the only way liquid rocket engines will be developed in the future.

Acknowledgments

The work performed by Aerojet and portions of the work performed by the Chemical Automatics Design Bureau were funded under the NASA Cooperative Agreement NCC8-44.

References

[1]"Access to Space—Advanced Technology Team: Final Report," Office of Space Systems Development, NASA Headquarters, Washington, DC, July 1993.

[2]Aldrich, A. D., "Access to Space Study, Summary Report," Office of Space Systems Development, NASA Headquarters, Washington, DC, Jan. 1994.

[3]Martin, J. A., "Effects of Tripropellant Engines on Earth-to-Orbit Vehicles," *Journal of Spacecraft and Rockets*, Vol. 22, No. 6, 1985, pp. 620–625.

[4]Bekey, I., "SSTO Rockets: A Practical Possibility," *Aerospace America*, July 1994, pp. 32–37.

[5]Martin, J. A., "History of Propulsion for SSTO and Multiple Stage Vehicles," AIAA Paper 93-1942, June 1993.

[6]Salkeld, R., "Mixed-Mode Propulsion for the Space Shuttle," *Astronautics and Aeronautics*, Vol. 9, No. 8, 1971, pp. 52–58.

[7]Wilhite, A. W., "Optimization of Rocket Propulsion Systems for Advanced Earth-to-orbit Shuttles," *Journal of Spacecraft and Rockets*, Vol. 17, No. 2, 1980, pp. 99–104.

[8]Martin, J. A., "A Method for Determining Optimum Phasing of a Multiphase Propulsion System for a Single-Stage Vehicle with Linearized Inert Weight," NASA TN-7792, 1974.

[9]Colasurdo, G., Pastrone, D., and Casalino, L., "Optimal Performance of a Dual-Fuel Single-Stage Rocket," *Journal of Spacecraft and Rockets*, Vol. 35, No. 5, 1998, pp. 667–671.

[10]Henry, B. V., and Decker, J. P., "Future Earth Orbit Transportation Systems/Technology Implications," *Astronautics and Aeronautics*, Vol. 14, No. 9, 1976, pp. 18–28.

[11]Wilhite, A. W., "Advanced Rocket Propulsion Technology Assessment for Future Space Transportation," *Journal of Spacecraft and Rockets*, Vol. 19, No. 4, 1982, pp. 314–319.

[12]Martin, J. A., "Hydrocarbon Rocket Engines for Earth-to-Orbit Vehicles," *Journal of Spacecraft and Rockets*, Vol. 20, No. 3, 1983, pp. 249–256.

[13]Martin, J. A., "Selecting Hydrocarbon Rocket Propulsion Technology," IAF-86-167, 37th Congress of the International Astronautical Federation, Innsbruck, Austria, 1986.

[14]Lepsch, R. A., Jr., Stanley, D. O., and Unal, R., "Dual-fuel Propulsion in Single-Stage Advanced Manned Launch System Vehicle," *Journal of Spacecraft and Rockets*, Vol. 32, No. 3, 1995, pp. 417–425.

[15]Kozlov, A. A., Hinckel, J. N., Koreeda, J., and Comiran, A., "Payload Evaluation of a Tripropellant Carrier Rocket," *Journal of Propulsion and Power*, Vol. 15, No. 2, 1999, pp. 304–309.

[16]Goracke, B. D., Levack, D. J. H., and Johnson, G. W., "Tripropellant Engine Option Comparison for Single Stage to Orbit," *Journal of Spacecraft and Rockets*, Vol. 34, No. 5, 1997, pp. 636–641.

[17]Stanley, D. O., Engelund, W. C., and Lepsch, R. A., "Propulsion System Requirements for Reusable Single-Stage-To-Orbit Rocket Vehicles," AIAA Paper 92-3504, 1992.

[18]Tkachenko, J. N., and Limerick, C. D., "Powerful Liquid Rocket Engine (LRE) Created by NPO Energomash for Up to Date Space Rockets," AIAA Paper 93-1957, 1993.

[19]Katorgin, B. I., Chelkis, F. J., and Limerick, C. D., "The RD-170, A Different Approach to Launch Vehicle Propulsion," AIAA Paper 93-2415, 1993.

[20]Lozino-Lozinsky, G. E., Shkadov, L. M., and Plokhikh, V. P., "Reusable Aerospace System with Horizontal Launch," *Space Technology*, Vol. 13, No. 1, 1993, pp. 11–23.

[21]Lozino-Lozinskaya, I. G., Chelkis, F. J., and Tanner, L. G., "The Current Status of Tripropellant Combustion Technology," *Proceedings of the Second International Symposium on Liquid Rocket Propulsion*, Chatillon, France, June 19–21, 1995.

[22]Visek, W. A., "LOX/Hydrocarbon Booster Engine Concepts," AIAA Paper 86-1687, 1986.

[23]Visek, W. A., "Design Concept for LOX/Hydrocarbon Tripropellant Booster Engine," AIAA Paper 87-1854, 1987.

[24]Yatsuyanagi, N., Sato, K., Sakamoto, H., Ono, F., and Tamura, H., "Stabilizing Effect of Hydrogen Injection on LOX/Kerosene Unstable Combustion," *Proceedings of the Seventeenth International Symposium on Space Technology and Science*, Tokyo, Japan, 1990.

[25]Yatsuyanagi, N., Sato, K., Sakamoto, H., and Ono, F., "Improvement of LOX-Kerosene Combustion Efficiency with Hydrogen Injection," *Proceedings of the Eighteenth International Symposium on Space Technology and Science*, Kagoshima, Japan, 1992.

[26]Ono, F., Tamura, H., Kumakawa, S., Sakamoto, H., Sato, K., Sasaki, M., and Yatsuyanagi, N., "Effects of Hydrogen Addition on Combustion Performance of a LOX/Kerosene Rocket," National Aerospace Laboratory, TR-1177, 1992.

[27]Kumakawa, S., Ono, F., and Yatsuyanagi, N., "Combustion and Heat Transfer of LO_2/HC/Hydrogen Tripropellant," AIAA Paper 95-2501, 1995.

[28]Clemons, K., Schmidt, M., Mouis, A. G. F., Ni, T., Pal, S., and Santoro, R. J., "Tripropellant Combustion using RP1/GO_2/GH_2: Drop and Injector Studies," *Proceedings of the 32nd JANNAF Combustion Subcommittee Meeting*, 1995, pp. 199–207.

[29]Rhys, N., and Hawk, C. W., "Tripropellant Combustion: Chemical Kinetics and Combustion Instability," AIAA Paper 95-3151, 1995.

[30]Ramamurthi, K., and Nair, G. M., "Coaxial Swirl Injection Element for a Tripropellant Engine," AIAA Paper 98-3514, 1998.

[31]Schmidt, M. G., and Micci, M. M., "Combustion Performance of RP-1/O_2/H_2 Tripropellants," AIAA Paper 98-3686, 1998.

[32]Qinglian, L., Yuhui, H., and Zhenguo, W., "The Numerical Simulation of the Hot Flow Field in Tripropellant LRE," AIAA Paper 01-3715, 2001.

[33]Rachuk, V., Matinenko, Y. A., Gontcharov, N. S., and Sciorelli, F., "Design, Development, and History of the CADB RD-0120 Engine," AIAA Paper 95-2540, 1995.

[34]Rudis, M. A., Orlov, V. A., Rachuk, V. S., Nikitin, L. N., and Campbell, W. E., "A Universal Methodology for Predicting Liquid Rocket Engine Durability Based on Russian RD-0120 Engine Operating Experience," AIAA Paper 95-2963, 1995.

[35]Lauston, M. F., Rousar, D. C., and Bucella, S., "Carbon Deposition with LOX/RP-1 Propellants," AIAA Paper 85-1164, 1985.

[36]Turtushov, V. A., Orlov, V. A., Yefremov, Y. A., Gontcharov, N. S., Hulka, J., and Dexter, C., "Development Status of a Soot-Free Fuel-Rich Kerosene Tripropellant Preburner for Reusable Liquid Rocket Engine Applications," AIAA Paper 95-3002, 1995.

[37]Turtushov, V. A., Orlov, V. A., Gontcharov, N. S., Yefremov, Y. A., Veremyenko, N. A., and Hulka, J., "Final Model Development and Full-Scale Testing of a Soot-Free Fuel-Rich Kerosene Tripropellant Preburner," AIAA Paper 96-2630, 1996.

[38]Orlov, V., Rachuk, V., Gontcharov, N. S., and Starke, R. G., "Reusable Launch Vehicle Propulsion Based on the RD-0120 Engine," AIAA Paper 95-3003, 1995.

[39]Rachuk, V. S., Shostak, A. V., Dmitrenko, A. I., Goncharov, G. I., Hernandez, R., Starke, R. G., and Hulka, J., "Benchmark Testing of an Enhanced Operability LO_2/LH2 RD-0120 Engine," AIAA Paper 96-2609, 1996.

[40]Rachuk, V., Orlov, V., Plis, A., Gontcharov, N., and Fanciullo, T. J., "The Low Risk Development of a Fuel-Rich Preburner Tripropellant Engine Using the RD-0120 Engine," AIAA Paper 94-9465, 1994.